Solid State Communications 250 (2017) 64–69

Contents lists available at ScienceDirect

Solid State Communications

journal homepage: www.elsevier.com/locate/ssc

Communication

First-principles investigation of the effect of charged unit cell on the electronic structure of two-dimensional MoS_2

Ashkan Shekaari*, Mohammad Reza Abolhassani, Hamed Lashgari

Plasma Physics Research Center, Science and Research Branch, Islamic Azad University, 14778-93855 Tehran, Iran

ARTICLE INFO

Keywords:
Two-dimensional MoS_2
Density-functional theory
Electronic properties

ABSTRACT

Density-functional theory has been applied to investigate the effect of charged unit cell on the structural and electronic properties of two-dimensional MoS_2 within PBE-GGA. The charge of the unit cell of the monolayer changes from zero to $n = \pm 4e$ with e the absolute value of the elementary electric charge. Variations of the lattice constant, Mo–S bond length, S–Mo–S bond angle, total energy, exchange and correlation contributions, and the Fermi level versus n have been calculated quantitatively, indicating decrease in the stability of the atomic structure of the monolayer with increase in the absolute value of n. It is found that the Fermi level for two-dimensional MoS_2 is a function of both the number of electrons in allowed states and the inverse of the volume of the unit cell. The electronic properties of each monolayer have been also calculated via examining the related electronic band structure and density of states. Results broadly support the view that the effect of charged unit cell ($n = +e$ to $-4e$) on the electronic properties of MoS_2 monolayer is manifested in the form of semiconductor-to-metal transition in addition to the Fermi level shift. It is also verified that as the negative charge of the unit cell increases from $n = -e$ to $-4e$, there is an ever-increasing trend in the total number of allowed electronic states at the Fermi level, implying a direct correlation between electrical conductivity and the value of n in a way that the more negative the charge of the unit cell, the higher the electrical conductivity of the monolayer.

1. Introduction

An important class of low-dimensional systems includes two-dimensional layered materials studied to reveal their fundamental chemistry and physics at the thickness of single atoms with a high potential for opening up new emerging technological opportunities and applications [1]. Amongst them is molybdenum disulfide having emerged as a new layer semiconducting material, been a subject of extensive studies, and attracted much attention because of the wide range of applications related to its finite, tunable, and direct band gap [2–7]. It has also been considered as an alternative to graphene mainly because of its large, intrinsic, direct band gap of about 1.8 eV [3], making it suitable for nanoelectronic and optoelectronic devices [5,6]. With such a band gap, conduction through the material could be tuned between *on* and *off* states—an important property graphene does not consist of. Two-dimensional MoS_2 demonstrates many intriguing physical properties including strong exciton binding energy [8], and valley selective circular dichroism [9–11], making it a novel material for next generation nanoelectronics [4] and photonics [12]. It has potential capabilities in thermoelectric energy conversion [13] and field-effect transistors (FETs), exhibiting high channel mobility ($200\ cm^2\ V^{-1}\ s^{-1}$) and high current *on*/*off* ratio (10^8) when it is used as channel material in FETs [4]. The absence of interface dangling bonds and easy fabrication through exfoliation methods have made it an important subject of studies in nanotechnology and logic devices [4].

Almost all functional aspects of two-dimensional MoS_2 in industry and technology include applying the monolayer—as substrate or on substrate—in contact with other materials such as heterojunction solar cells [14], FETs [15], transistors with ionic-liquid gating [16], etc. In such cases, therefore, the contact between MoS_2 monolayer and other materials, and so the possible difference between their electronegativities could result in the important case of MoS_2 monolayer with charged unit cell: a case which has not yet been studied.

Therefore, in the present work, the effect of charged unit cell on the electronic structure of two-dimensional MoS_2 is going to be investigated within the framework of density-functional theory and PBE-GGA. The charge of the unit cell changes from $n = -4e$ to $+4e$ with e the absolute value of the elementary electric charge. The electronic structure of the resulted $(MoS_2)^n$ monolayers are then calculated via

* Corresponding author.
E-mail address: shekaari@gmail.com (A. Shekaari).

http://dx.doi.org/10.1016/j.ssc.2016.11.016
Received 12 May 2016; Received in revised form 29 October 2016; Accepted 16 November 2016
Available online 20 November 2016
0038-1098/

examining the related electronic band structures and density of states (DOS), being compared to those of the neutral monolayer (n=0). The stabilities of the atomic structures of the monolayers are also discussed via evaluating the related Mo–S bond lengths, S–Mo–S bond angles, and internal energies.

2. Computational method

Density-functional theory has been applied to investigate the effect of charged unit cell on the structural and electronic properties of graphene-like, hexagonal MoS_2 monolayer using self-consistent plane wave pseudopotential method as implemented in the Quantum ESPRESSO integrated suite [17]. The generalized gradient approximation (GGA) proposed by Perdew, Burke and Ernzerhof (PBE) [18] has been applied for the exchange and correlation functionals of all monolayers. Effects of the core (non-valence) electrons of the two atomic species have been described using scalar-relativistic ultrasoft pseudopotentials generated by Rappe–Rabe–Kaxiras–Joannopoulos (RRKJ) pseudization method with nonlinear core correction [19,20]. The valence shells are considered to be 3s3p for S atoms and 4s4p4d5s for Mo atom. The kinetic energy cut-off of about 952 eV for the wave functions, and 4082 eV for the charge densities and the potentials have been found to be enough to reach energy convergence. The primitive cell containing one Mo atom and two S atoms in graphene-like, hexagonal Bravais lattice has been used under periodic boundary conditions (Fig. 1). The vacuum spaces along the z-axis ranging from 24.50 Å (for $n=+e$) to 27.07 Å (for $n=-4e$) have been calculated to be enough to decouple the weakest possible periodic interactions. The Brillouin zone is sampled along Γ, M, K, Γ by 163 k-points using the Methfessel–Paxton smearing method [21]. The unit cell of each monolayer has been relaxed using Murnaghan's isothermal equation of state, applying uniform strain to the unit cell and finds its equilibrium, zero-pressure lattice constant (a_0). After variable-cell relaxation, a fixed-cell relaxation based upon the Broyden–Fletcher–Goldfarb–Shanno optimization method (BFGS) is performed on the atomic positions of each monolayer in order to find the relaxed atomic positions in a way that the magnitude of the total force on each atom drops to less than 1.8×10^{-4} eV/Å. The type of the smearing method, and the value of the Gaussian spreading for Brillouin-zone integrations have been also tested to reach energy convergence.

Table 1
The values of the equilibrium lattice parameter (a_0), Mo–S bond length, S–Mo–S bond angle, and the volume of the unit cell (Ω) for each monolayer.

n	a_0 (Å)	Mo–S (Å)	S–Mo–S (°)	Ω (Å^3)
$+2e$	2.9544	5.5831	144.421	178.5912
$+e$	3.0631	2.4421	87.199	199.0465
0	3.1705	2.4109	81.198	220.7194
$-e$	3.3568	2.4346	74.487	261.9638
$-2e$	3.3833	2.4450	73.944	268.2197
$-3e$	3.3839	2.4701	75.453	268.3456
$-4e$	3.3846	2.4750	75.714	268.5219

3. Results and discussion

3.1. Structural parameters and energy

In the following, the values of the lattice constant, Mo–S bond length, and S–Mo–S bond angle are going to be calculated for each n from zero to $\pm$ 4e. For this end, a variable-cell relaxation based upon the Murnaghan's isothermal equation of state is performed on each monolayer, which applies a uniform strain to the unit cells and then finds their zero-pressure lattice parameter. After having the true lattice constants, a fixed-cell relaxation—the BFGS method—is applied to compute the relaxed atomic positions, giving the equilibrium Mo–S bond lengths, and S–Mo–S bond angles tabulated in Table 1.

It is seen that as the charge of the unit cell becomes more negative (from $n=+2e$ to $-4e$), its lattice parameter becomes larger, and vice versa, the more positive the charge of the unit cell, the smaller the lattice parameter. Such a trend holds also for $n=+3e$ and $+4e$, but the cases with $n=+2e$, $+3e$, and $+4e$ have to be ignored because of very large values of their equilibrium Mo–S bond lengths and S–Mo–S bond angles—indicating either the atomic structures of these monolayers collapse or their inter-atomic bonds are broken. Our considerations, therefore, have to be limited to the cases with n ranging from $+e$ to $-4e$. For the equilibrium Mo–S bond length, the minimum value is that of the neutral monolayer (n=0), while for the rest of monolayers there exists an ever-increasing trend with increase in the absolute value of n. Examining the equilibrium S-Mo-S bond angles indicates no explicit pattern for their variation versus n. Considerations related to energy represent a trend for variation of the total energy (E_{tot}) of the monolayer versus n similar to that of the Mo-S bond length in a way that the minimum value of E_{tot} is that of the neutral monolayer—the

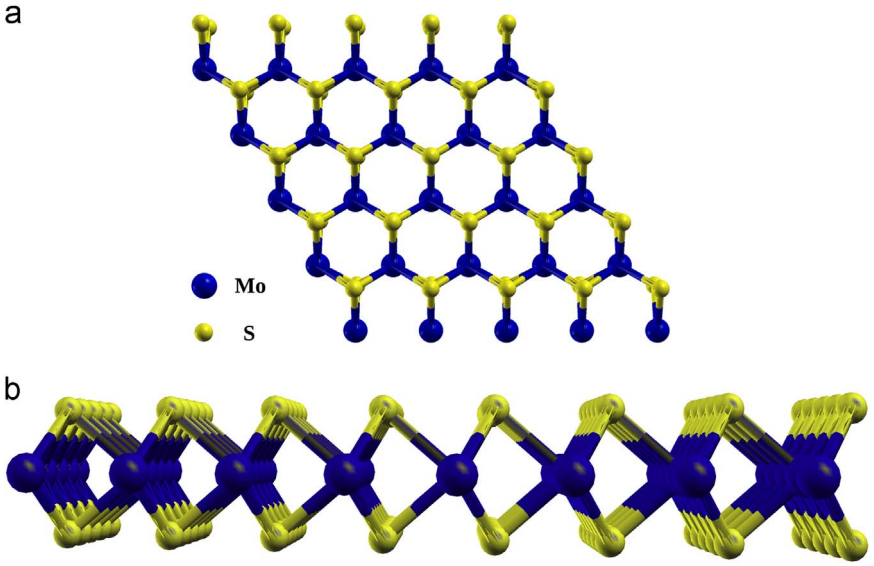

Fig. 1. Atomic structure of two-dimensional MoS_2 in graphene-like, hexagonal Bravais lattice: (a) top view (in x–y plane) of 5×5 unit cells, (b) side view (arm-chair). Layers of Mo atoms are sandwiched between S atoms in a way that each Mo is bonded to six S.

Table 2
Values of E_{tot}, E_F, E_X, and E_C for each monolayer calculated using self-consistent-field method.

n	E_{tot} (eV)	E_F (eV)	E_X (eV)	E_C (eV)
$+e$	−2619.2389	−24.5116	−529.0902	−39.9762
0	−2632.3948	−0.9384	−538.2598	−41.1710
$-e$	−2631.7431	0.5191	−541.6837	−41.6858
$-2e$	−2631.3955	0.3158	−545.8578	−42.4361
$-3e$	−2631.0606	0.3162	−549.9504	−43.2511
$-4e$	−2630.7208	0.4080	−554.9233	−44.2103

most stable monolayer. As the charge of the unit cell becomes more positive or more negative (compared to n=0), E_{tot} increases and implies that the stability of the atomic structure of the monolayer is being reduced. The values of E_{tot}, the Fermi energy (E_F), and exchange (E_X) and correlation (E_C) energies are tabulated in Table 2 for each monolayer.

Although E_{tot} becomes more positive with increase in the absolute value of n, E_X and E_C decrease as the charge of the unit cell becomes more negative from $n=+e$ to $-4e$. Such a result is generally expected and shows that E_X and E_C tend to stabilize the atomic structure of the system. That E_{tot} becomes more positive with increase in the negative charge of the unit cell indicates that the Coulomb repulsion between electrons overcomes the stabilizer contributions of the exchange and correlation so that its overall effect could be manifested as increase in

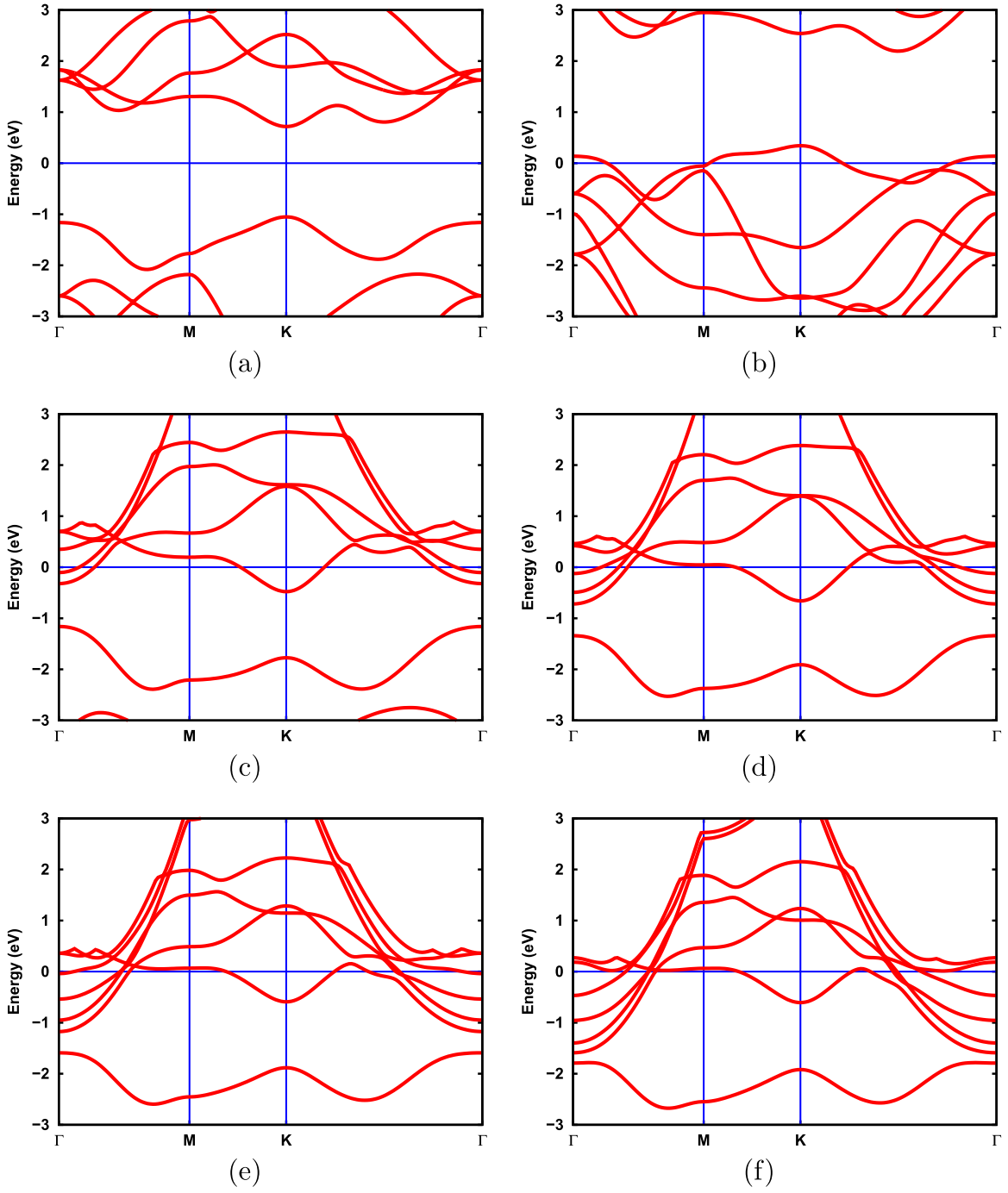

Fig. 2. The calculated electronic band structures of two-dimensional $(MoS_2)^n$ for (a) n=0, (b) $n=+e$, (c) $n=-e$, (d) $n=-2e$, (e) $n=-3e$, and (f) $n=-4e$.

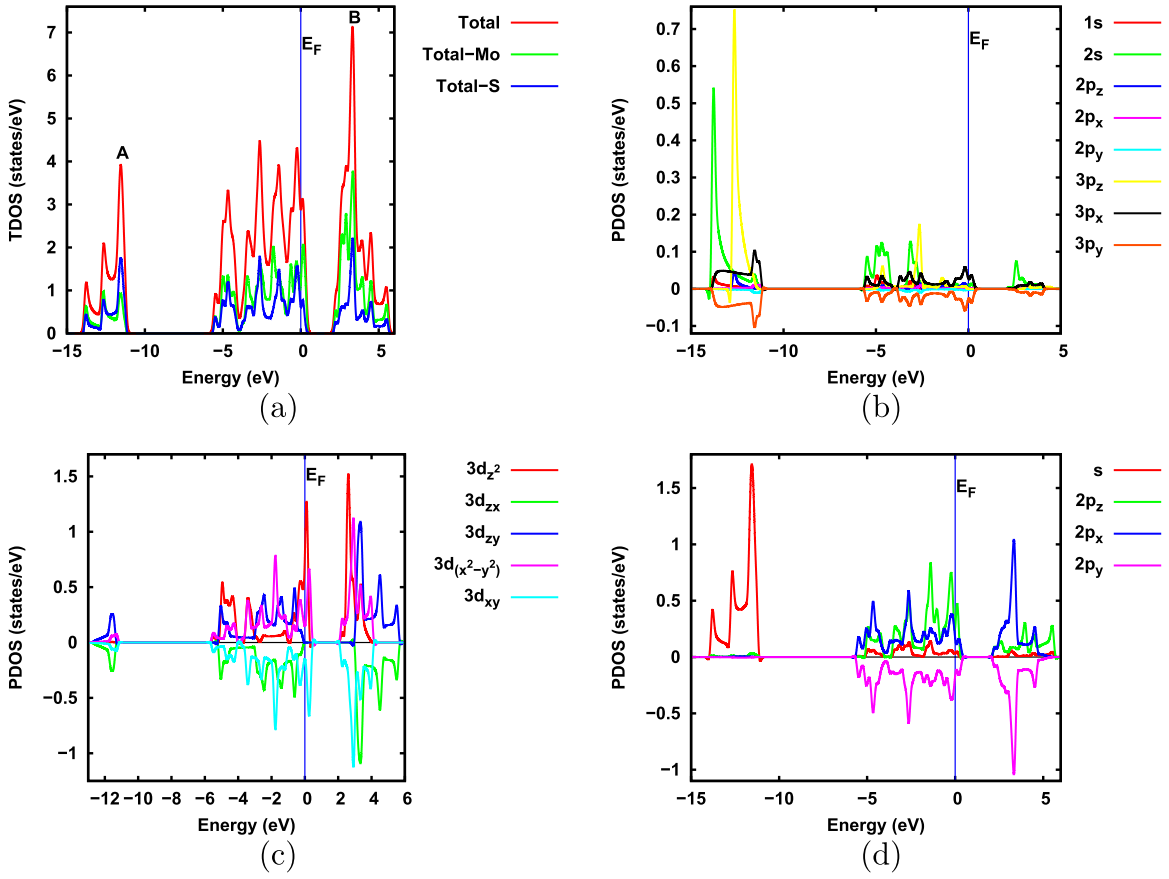

Fig. 3. The calculated DOS for $n=+e$: (a) TDOS for $(MoS_2)^{+e}$ monolayer, Mo atom, and S atoms, (b) PDOS for Mo (contributions of the s- and p-orbitals), (c) PDOS for Mo (contributions of the 3d-orbitals), and (d) PDOS for S.

E_{tot} and so destabilizes the system. As expected–and it has been generally known by theory–the correlation contributions to the E_{tot}s are much smaller than those of the exchange [22,23].

3.2. Electronic properties

Being examined the related electronic band structures and DOS, the electronic properties of two-dimensional MoS_2 with charged unit cell are extensively investigated within the framework of density-functional theory and PBE-GGA. The aim is to determine the way these electronic properties evolve as the charge of the unit cell changes from $n=+e$ to $-4e$.

The values included in Table 2 verify that the Fermi level shifts from the valence band (VB) to the conduction band (CB) (from negative to positive values) as the number of electrons of the neutral unit cell increases. Such an outcome, indeed, is expected because the addition of electrons yields increase in the number of electronic states to be occupied and consequently shifts the Fermi level upward. As seen in Table 2, the increasing trend of E_F is interestingly violated for $n=-2e$ and $-3e$ because in such cases, both the number of electrons available in the unit cell and its volume increase (Table 1) compared to $n=-e$ but with higher increase in the volume so that E_F is reduced. As a consequence, it could be deduced that the Fermi level for two-dimensional MoS_2 is a function of both the number of electrons in allowed states and the inverse of Ω, just in accord with the known formula below for the Fermi level:

$$E_F = \left(3\pi^2 \frac{N_0}{\Omega}\right)^{\frac{2}{3}} \frac{\hbar^2}{2m_e}$$

with N_0 the number of electrons in allowed states and m_e the mass of an electron [24].

Fig. 2 illustrates the band structures of two-dimensional $(MoS_2)^n$ for $n=+e$ to $-4e$. The Brillouin-zone integrations have been carried out along Γ, M, K, Γ. As seen in Fig. 2a, the valence band maximum (VBM) and the conduction band minimum (CBM) are located at the K-point as expected, exhibiting the semiconducting property of two-dimensional $(MoS_2)^0$ with a direct K–K gap of about 1.76 eV.

From Fig. 2b, showing the band structure of $(MoS_2)^{+e}$, it is seen that the pattern of VBM-CBM at the K-point obtained for n=0 does not hold anymore and the Fermi level shifts downward to the VB because of losing an electron from the unit cell, which consequently decreases the number of electronic states to be occupied. In addition to the Fermi level shift, the energy bands intersect the Fermi level, indicating the semiconductor-to-metal transition for $(MoS_2)^{+e}$. In such a case, because of losing an electron, the VB is partially filled, and so electrons could move more easily, be transmitted to the CB, and conduct electricity well. Such transition could be also seen in the electronic partial DOS (PDOS) and total DOS (TDOS) diagrams as illustrated in Fig. 3, showing how the allowed electronic states are filled.

As seen in Fig. 3a, the TDOS of $(MoS_2)^{+e}$ monolayer intersects the Fermi level at about 2.8866 (states/eV), approving its electrical conducting property obtained via the related band structure. Examining the other subfigures demonstrates that the peak of 3.921 (states/eV) at −11.547 eV (peak A) is mainly caused by the s-orbitals of S, and trivially by the $3p_x$- and $3p_y$-orbitals of Mo. Also, the peak of 7.132 (states/eV) at 3.322 eV (peak B) is mainly related to the $3d_{zx}$- and $3d_{zy}$-orbitals of Mo, and to the $2p_x$- and $2p_y$-orbitals of S. As is seen, the $3d_{zx}$- and $3d_{zy}$-orbitals, the $3d_{x^2-y^2}$- and $3d_{xy}$-orbitals, the $2p_x$- and $2p_y$-orbitals, and the $3p_x$- and $3p_y$-orbitals of Mo, and the $2p_x$- and $2p_y$-orbitals of S have equal contributions to the TDOS two-by-two.

From Fig. 2 it is seen that for the monolayers with negative-charged

Table 3
The calculated TDOS at the Fermi level as well as the values and positions of the peaks A and B for two-dimensional $(MoS_2)^n$ for $n = 0, -e, -2e, -3e$, and $-4e$.

n	TDOS at E_F	Peak A		Peak B	
	(states/eV)	(states/eV)	(eV)	(states/eV)	(eV)
0	0.000	4.718	−13.264	5.545	1.735
$-e$	2.562	3.730	−13.768	8.010	0.624
$-2e$	4.801	3.776	−13.985	7.279	0.429
$-3e$	6.004	3.635	−14.047	7.868	0.329
$-4e$	6.627	3.599	−14.171	8.025	0.111

unit cell ($n = -e$ to $-4e$) the pattern of VBM-CBM at the K-point obtained for n=0 is not hold anymore and E_F shifts upward to the CB (Table 2) because of adding electrons to the unit cell, which consequently increases the number of electronic states to be occupied. In addition to the Fermi level shifts in such cases, the energy bands of the monolayers intersect the Fermi level, indicating semiconductor-to-metal transition for the monolayers. Indeed, because of increase in the negative charge of the unit cell, the VB overlaps the CB, and consequently results in electronic transmissions between the two bands. Such electronic transmissions obtained for $n = +e, -e, -2e, -3e$, and $-4e$ are actually happened at absolute zero (T=0 K), and therefore, at room temperature (0.025 eV), more electrical conducting property is expected for the monolayers because of the ionization of electrons to the CB.

The results obtained via examining the PDOS and TDOS of $(MoS_2)^{+e}$ are also valid for $n = -e$ to $-4e$ in a way that the same orbitals have contributions to the peaks A and B, but for each monolayer, the peaks occur at different energies and their TDOS diagrams intersect the Fermi level at different points, as tabulated in Table 3.

Interestingly, it is seen that the total density of states at the Fermi level increases with increase in the negative charge of the unit cell from zero to $n = -4e$, implying the direct correlation between electrical conductivity and the value of n in a way that the more negative the charge of the unit cell, the higher the electrical conductivity of the monolayer. Also, with increase in the negative value of n, the energies the peaks A and B occur at decrease and shift leftward to the negative side of the E-axis proportional to the shifts in E_F as expected.

4. Conclusions

In the present work, the effect of charged unit cell on the electronic structure of two-dimensional MoS_2 has been calculated quantitatively within the framework of density-functional theory and PBE-GGA. The charge of the unit cell changes from $n = +e$ to $-4e$ with e the absolute value of the elementary electric charge. Variations of the structural properties versus n are obtained via calculating the related lattice parameter, Mo–S bond length, S–Mo–S bond angle, E_{tot}, E_F, E_X, and E_C. The electronic properties of $(MoS_2)^n$ monolayers with charged unit cell are then investigated via examining the related electronic band structures and PDOS. In summary, results verify that: (i) as the charge of the unit cell becomes more negative, its lattice parameter becomes larger, and vice versa, the more positive the charge of the unit cell, the smaller the lattice parameter; (ii) for the equilibrium Mo-S bond length, the minimum value is that of the neutral monolayer (n=0), and for the rest of monolayers, there is an ever-increasing trend with increase in the absolute value of n; (iii) the minimum value of E_{tot} is that of the neutral monolayer in a way that as the charge of the unit cell becomes more positive or more negative (compared to n=0), E_{tot} increases, implying decrease in the stability of the atomic structure of the monolayer with increase in the absolute value of n; (iv) E_X and E_C decrease as the charge of the unit cell becomes more negative from $n = +e$ to $-4e$; (v) the Fermi level for two-dimensional MoS_2 is a function of both the number of electrons in allowed states and the inverse of the volume of the unit cell; (vi) for $n = +e$, the pattern of VBM-CBM at the K-point obtained for n=0 does not hold, and in addition to shift in E_F downward to the VB, the energy bands intersect the Fermi level, indicating semiconductor-to-metal transition for the monolayer at absolute zero; (vii) for negative-charged unit cells ($n = -e$ to $-4e$) the pattern of VBM-CBM at the K-point obtained for the neutral unit cell does not hold and in addition to the shifts in E_F upward to the CB, energy bands intersect the Fermi level, implying semiconductor-to-metal transition for the monolayers; (viii) for all monolayers with charged unit cells, their TDOS diagrams intersect the Fermi level, approving their semiconductor-to-metal transitions obtained via the band structure considerations; (ix) as the negative charge of the unit cell increases from zero to $n = -4e$, the TDOS at the Fermi level increases too, indicating direct correlation between electrical conductivity and the value of n in a way that the more negative the charge of the unit cell, the higher the electrical conductivity of the monolayer.

References

[1] X. Duan, C. Wang, A. Pan, R. Yu, X. Duan, Two-dimensional transition metal dichalcogenides as atomically thin semiconductors: opportunities and challenges, Chem. Soc. Rev. 44 (2015) 8859–8876.
[2] J.W. Jiang, arXiv:1408.0434v1.
[3] K.F. Mak, C. Lee, J. Hone, J. Shan, T.F. Heinz, Atomically thin MoS_2: A new direct-gap semiconductor, Phys. Rev. Lett. 105 (2010) 136805–136809.
[4] B. Radisavljevic, A. Radenovic, J. Brivio, V. Giacometti, A. Kis, Single-layer MoS_2 transistors, Nat. Nanotechnol. 6 (2011) 147–150.
[5] Q.H. Wang, K. Kalantar-Zadeh, A. Kis, J.N. Coleman, M.S. Strano, Electronics and optoelectronics of two-dimensional transition metal dichalcogenides, Nat. Nanotechnol. 7 (2012) 699–712.
[6] M. Chhowalla, H.S. Shin, G. Eda, L.J. Li, K.P. Loh, H. Zhang, The chemistry of two-dimensional layered transition metal dichalcogenide nanosheets, Nat. Chem. 5 (2013) 263–275.
[7] A. Splendiani, L. Sun, Y. Zhang, T. Li, J. Kim, C.Y. Chim, G. Galli, F. Wang, Emerging photoluminescence in monolayer MoS_2, Nano Lett. 10 (2010) 1271–1275.
[8] D.Y. Qiu, F.H. daJornada, S.G. Louie, Optical spectrum of MoS_2: Many-body effects and diversity of exciton states, Phys. Rev. Lett. 111 (2013) 216805–216809.
[9] T. Cao, G. Wang, W. Han, Valley-selective circular dichroism of monolayer molybdenum disulphide, Nat. Commun. 3 (2012) 887–892.
[10] K.F. Mak, K.L. He, J. Shan, T.F. Heinz, Control of valley polarization in monolayer MoS_2 by optical helicity, Nat. Nanotechnol. 7 (2012) 494–498.
[11] H.L. Zeng, J. Dai, W. Yao, D. Xiao, X. Cui, Valley polarization in MoS_2 monolayers by optical pumping, Nat. Nanotechnol. 7 (2012) 490–493.
[12] O. Lopez-Sanchez, D. Lembke, M. Kayci, A. Radenovic, A. Kis, Ultrasensitive photodetectors based on monolayer MoS_2, Nat. Nanotechnol. 8 (2013) 497–501.
[13] M. Buscema, M. Barkelid, V. Zwiller, H.S.J. van der Zant, G.A. Steele, A. Castellanos-Gomez, Large and tunable photothermoelectric effect in single-layer MoS_2, Nano Lett. 13 (2013) 358–363.
[14] M.L. Tsai, S.H. Su, J.K. Chang, D.S. Tsai, C.H. Chen, C.I. Wu, L.J. Li, L.J. Chen, J.H. He, MoS_2 monolayer heterojunction solar cells, ACS Nano 8 (2014) 8317–8322.
[15] W. Bao, X. Cai, D. Kim, K. Sridhara, M.S. Fuhrer, High mobility ambipolar MoS_2 field-effect transistors: substrate and dielectric effects, Appl. Phys. Lett. 102 (2013) 042104–042116.
[16] M.M. Perera, M.W. Lin, H.J. Chuang, B.P. Chamlagain, C. Wang, X. Tan, M.M. Cheng, D. Tománek, Z. Zhou, Improved carrier mobility in few-layer MoS_2 field-effect transistors with ionic-liquid gating, ACS Nano 7 (2013) 4449–4458.
[17] P. Giannozzi, S. Baroni, N. Bonini, M. Calandra, R. Car, C. Cavazzoni, D. Ceresoli, G.L. Chiarotti, M. Cococcioni, I. Dabo, A.D. Corso, S. de Gironcoli, S. Fabris, G. Fratesi, R. Gebauer, U. Gerstmann, C. Gougoussis, A. Kokalj, M. Lazzeri, L. Martin-Samos, N. Marzari, F. Mauri, R. Mazzarello, S. Paolini, A. Pasquarello, L. Paulatto, C. Sbraccia, S. Scandolo, G. Sclauzero, A.P. Seitsonen, A. Smogunov, P. Umari, R.M. Wentzcovitch, QUANTUM ESPRESSO: a modular and open-source software project for quantum simulations of materials, J. Phys.: Cond. Matter 21 (2009) 395502–395521.
[18] J.P. Perdew, K. Burke, M. Ernzerhof, Generalized gradient approximation made simple, Phys. Rev. Lett. 77 (1996) 3865–3868.

[19] A.M. Rappe, K.M. Rabe, E. Kaxiras, J.D. Joannopoulos, Optimized pseudopotentials, Phys. Rev. B 41 (1990) 1227–1230.
[20] S.G. Louie, S. Froyen, M.L. Cohen, Nonlinear ionic pseudopotentials in spin-density-functional calculations, Phys. Rev. B 26 (1982) 1738–1742.
[21] M. Methfessel, A.T. Paxton, High-precision sampling for Brillouin-zone integration in metals, Phys. Rev. B 40 (1989) 3616–3621.
[22] J. Kohanoff, Electronic Structure Calculations for Solids and Molecules: Theory and Computational Methods, First ed., Cambridge University Press, Cambridge, 2006.
[23] R.G. Parr, W. Yang, Density-Functional Theory of Atoms and Molecules, Oxford University Press, New York, Oxford, 1989.
[24] E.A. Irene, Electronic Materials Science, John Wiley & Sons, Hoboken, New Jersey, 2005.